



# Reinforcement of biodegradable SiO<sub>2</sub>NPs-modified cellulose-gelatin hydrogel films with antioxidant and antibacterial properties as potential food packaging composite

Sadia Sagar<sup>1</sup> · Umair Khalid<sup>2</sup> · Waqar Azim<sup>3</sup> · Maria Kanwal<sup>4</sup> · Nazia Hossain<sup>5</sup>

Received: 24 December 2023 / Accepted: 21 March 2024  
© The Author(s) 2024

## Abstract

This study proposed an innovative approach to the development of sustainable and biodegradable food packaging materials by incorporating inexpensive nano-silica (SiO<sub>2</sub>NPs) in designed hydrogel (CSG) film employing biodegradable polymers: synthetic polymer polyvinyl alcohol (PVA), natural polymer - carboxymethyl cellulose (CMC) and protein-based bio-polymer –gelatine, and a commercial crosslinker, tetraethoxysilane (TEOS) through a conventional air-dry casting technique. The CSG hydrogel blends were modified with varying amounts of SiO<sub>2</sub>NPs (0.05g, 0.1g, 0.15g and 0.2g) and compared with the blend without SiO<sub>2</sub>NPs to determine the effect of SiO<sub>2</sub>NPs loading through various characterisation techniques and applications including antioxidant and antimicrobial activity. Comprehensive characterizations of the CSG films revealed that CSG 0.1 (containing 0.1g SiO<sub>2</sub>NPs) exhibited the most favourable functional properties, low crystallinity, high flexibility, suitable pore size, thermal stability, adequate tensile strength, elongation at the breaking point and maximum stability by swelling and diffusion test. The addition of SiO<sub>2</sub>NPs consistently enhanced thermal and mechanical stability in all CSG films. Further, these CSG films were implemented for antioxidant test and antimicrobial activity against gram-positive *Bacillus cereus* and gram-negative *Escherichia coli*. SiO<sub>2</sub>NPs integration significantly elevated the antioxidant capacity in all films, with CSG 0.1 showing ~7% improvement. The antimicrobial activity of SiO<sub>2</sub>NPs-modified CSG films was also notable, with CSG 0.1 effectively inhibiting *B. cereus* by 1.2cm zone and *E. coli* by 0.5cm zone. A soil burial test was performed to pattern the biodegradability of CSG hydrogels. Therefore, the outstanding improvements in the intrinsic properties of CSG films, owing to SiO<sub>2</sub>NPs modification, positioned these CSG hydrogels as promising candidates for advanced food packaging materials in various industries.

**Keywords** Nano-reinforcement · Hydrogel film formation · Biodegradability · Antibacterial activity · Antioxidant activity · Food packaging material

## Abbreviations

CSG Nano silica in designed hydrogel

PVA Poly vinyl alcohol

CMC Carboxymethylcellulose

TEOS Tetraethoxysilane

XRD X-ray Diffraction technique

SEM Scanning electron microscope

TGA Thermogravimetric analysis

DTA Differential Thermal analysis

UTS Ultimate Tensile Strength

DCPIP 2,6-Dichlorophenolindophenol

✉ Nazia Hossain  
nazia.hossain@rmit.edu.au; bristy808.nh@gmail.com

<sup>1</sup> Department of Physics, Lahore Garrison University, Lahore, Pakistan

<sup>2</sup> Department of Physics, The University of Lahore, Lahore, Pakistan

<sup>3</sup> South Eastern Regional College, Downpatrick, Ireland, UK

<sup>4</sup> School of Chemistry, University of the Punjab, Lahore, Pakistan

<sup>5</sup> School of Engineering, RMIT University, Melbourne, VIC 3001, Australia

## Introduction

Exploration of sustainable food packaging materials is one of the high demand research areas globally due to the recent sustainable movement in packaging industries. Conventional packaging material containing plastics exhibits detrimental

characteristics comprising hazardous chemicals and degradation into micro and nano-plastic causing serious contamination of soil and water bodies and also posing challenges for proper disposal/plastic waste management. Consequently, in the quest for more sustainable alternatives, materials such as textiles and paper have emerged as viable options for packaging though these options have numerous limitations such as easy penetration of liquid and less stability. On the other hand, glass or metal-based packaging is heavy-weight and requires high processing costs for production. Therefore, biodegradable polymer-based packaging materials are highly desired due to their advantageous characteristics (e.g., transparency, low weight, tear resistance, stiffness, the ability to be air and heat-sealed, and a high strength-to-weight ratio) to resolve environmental concerns as well as economical [1–4]. The food industries have also embraced the application of nanotechnology by utilizing engineered nanoparticles to enhance the quality of their products by enhancing the performance of polymers for food packaging applications by improving their mechanical strength, swelling behaviour, thermal characteristics, and biodegradability [4]. Among the advancements, hydrogels comprising polymers have emerged as a notable option due to their ability to absorb water and other liquids, reaching a maximum capacity of their weight [4, 5]. Therefore, this study proposed a novel SiO<sub>2</sub>NPs in designed hydrogel (CSG) film as an active food packaging material. Biodegradable synthetic polymers PVA, along with natural polymer CMC played a significant role as important and biocompatible materials in food packaging industries for decades due to their sustainable and antimicrobial characteristics [6–8]. CMC-containing carboxymethyl groups (-CH<sub>2</sub>-COOH) are attached to certain hydroxyl (-OH) groups of the glucopyranose monomers comprising the cellulose backbone and serve as a viscosity modifier or thickener in food products and function as an emulsion stabilizer in various goods (including ice cream), non-food items such as toothpaste, laxatives, diet pills, water-based paints, detergents, textile sizing, reusable heat packs, and various paper products [6]. Gelatin, derived primarily from bovine collagen obtained from animal skin, bones, and connective tissues, results in a collection of peptides and proteins and is used as a gelling agent in various industries including food, beverages, pharmaceuticals, vitamin and medication capsules, photographic films and papers, and cosmetics [9, 10]. SiO<sub>2</sub>NPs, also known as silica nanoparticles or nano-silica, possess favourable characteristics such as good biocompatibility, low toxicity, thermal stability, and ease of synthesis, making them promising for various biological applications and a high potential candidate for food packaging material [11, 12]. TEOS is the ethyl ester of orthosilicic acid, Si(OH)<sub>4</sub> and is predominantly used in the semiconductor as well as packaging industries as

a crosslinking agent in silicone polymers and as a precursor for SiO<sub>2</sub> and various applications such as coatings for carpets, production of aerogel as an additive in alcohol-based rocket fuels to reduce heat flow to the chamber wall in regeneratively cooled engines [13–15]. In this study, the preparation of CSG films utilising biodegradable polymers: synthetic polymer - PVA, natural polymer - CMC and protein-based biopolymer - gelatine, nano-compound - SiO<sub>2</sub>NPs and a commercial crosslinker, TEOS were achieved through a simple conventional air-dry casting technique as sustainable and biodegradable food packaging material. This study aims to fabricate SiO<sub>2</sub>NP-modified hydrogel-based CSG films as active food packaging materials addressing essential needs related to health, environment, and food industries. The objective of this research is to develop a novel polymeric film, SiO<sub>2</sub>NP-modified CSG film for food packaging purposes which consists of non-toxic polymers and possesses biodegradable properties, allowing for easy decomposition. There have been very limited studies performed on engineered hydrogel composite for active food packaging in the literature so far. A related experimental study on engineered gelatine/cellulose-silver nanoparticles (AgNPs) modified nanocomposite presented a high potential of antibacterial activities against *E. coli* and *B. cereus* as active food packaging material [2]. Compared to earlier studies, the material composition for the current study is unique, readily available and inexpensive compared to expensive materials like AgNPs, and carbon nanotubes (CNTs) [2, 16]. Also, the antibacterial (against *E. coli* and *B. cereus*) and antioxidant (against free radical of 2,6-dichlorophenolindophenol (DCPIP)) activities of the proposed active composite have been explored in this study. Then, the novelty of this study is to fabricate a new blend of composite material, SiO<sub>2</sub>NP-modified CSG film containing gelatin-PVA-CMC-SiO<sub>2</sub>NPs-TEOS as active food packaging material and explore the improvement of intrinsic properties as well as antibacterial and antioxidant properties. The thermal and mechanical stability, swelling and diffusion characteristics and micro graphical orientation of this novel SiO<sub>2</sub>NP-modified CSG film have been explored comprehensively in this study to determine whether this composite will be competitive for commercial packaging materials or not.

## Materials and Methods

### Materials

PVA (purity: >98%), CMC (purity: >98%), TEOS (purity: 98.5%), gelatin, SiO<sub>2</sub> NPs (purity: >99.98%), ethanol (100%), and 2, 2-dichloro phenol indophenol

(DCPIP) (100%), as vitamin C source namely ascorbic acid) were purchased from Sigma-Aldrich, United Kingdom.

### Synthesis Methods of Hydrogel Film Preparation

The hydrogel film preparation has been used in this study is casting and blending method since it is well-established, user friendly, cost-effective method and all the control parameters can be maintained precisely throughout this technique [14]. To prepare the composite film, 0.1g of PVA was dissolved in 30mL of preheated distilled water through continuous stirring on a hot plate with a magnetic stirrer at a temperature of 60°C until complete dissolution. Similarly, 0.4g of gelatine and 0.6g of CMC were separately dissolved in 30mL and 40mL of distilled water, respectively, using continuous stirring on a hot plate at 60°C with a magnetic stirrer until complete dissolution. Subsequently, the PVA solution was added to the gelatine solution on the hot plate and mixed for 1h. After the 1h blending period, this PVA-gelatine solution was added to the CMC solution and blended for an additional 1h at 60°C. SiO<sub>2</sub>NPs were dispersed in 30mL of distilled water and subjected to sonication using a digital ultrasonic cleaner for 0.5h at room temperature. The sonicated SiO<sub>2</sub>NPs were then added to the PVA/CMC/gelatine solution and mixed for 0.5h. Furthermore, 100µL of TEOS (dissolved in 20mL of ethanol (C<sub>2</sub>H<sub>5</sub>OH)) was added dropwise as a crosslinker, followed by stirring for 3h at 60°C. The prepared solution was poured into Petri dishes to obtain film samples, which were then dried at room temperature for the next 3h. The dried film samples were peeled and placed in a desiccator within polythene packets for further study. Additionally, a control sample of the film was synthesized for comparison purposes. The code and composition of the synthesized hydrogel base film samples are given in Table 1. The schematic representation of preparing hydrogel film is given in Fig. 1.

**Table 1** The codes and compositions of PVA/CMC/gelatin films

Sample Codes	PVA(g)	CMC(g)	Gelatin(g)	SiO <sub>2</sub> NPs(g)	TEOS(µL)
CSG	0.1	0.6	0.4	0	100
CSG 0.05	0.1	0.6	0.4	0.05	100
CSG 0.1	0.1	0.6	0.4	0.10	100
CSG 0.15	0.1	0.6	0.4	0.15	100
CSG 0.2	0.1	0.6	0.4	0.20	100

## Characterizations

### Fourier Transforms Infrared Spectroscopy (FTIR)

Fourier transform infrared spectrometry was used to investigate the functional groups of the hydrogels. The scanning was performed by Agilent Technologies Cary 630 FTIR with the range of wavelength from 4000-650cm<sup>-1</sup> and the resolution was 4.0cm<sup>-1</sup>.

### X-Ray Diffraction (XRD) Techniques

XRD analysis of hydrogel film samples was performed by an X-ray Diffraction machine (STOE, Japan) with scan step: 0.25, scan speed: 1°/minute and scan angle: 10-80 at 2θ. XRD analysis is useful for the estimation of the structure characterization of thin films. X-ray diffraction gives the material's molecular structure and estimates the dispersion of doped particles in the structure of the sample.

### Scanning Electron Microscopy (SEM)

The samples were gold (Au) sputtered to make the samples conductive for the electron beam interaction. SEM analysis was performed to observe the surface morphology of synthesized hydrogel film samples. Scanning Electron Microscope (SEM, JSM, JEOL, Japan) was used to investigate the prepared dried films. Images were collected by using a scanning electron microscope at the magnification of 50 and 20µm.

### Thermogravimetric/Differential Thermal Analysis (TG/DTA)

Thermogravimetric analysis was performed to estimate the thermal behaviour of the CSG hydrogel film series. The thermal decomposition activity of samples was investigated in an air environment with and heating rate of 10°C/min from 29 to 816°C with a TG/DTG instrument (Perkin Elmer Diamond TG/DTA instrument, Japan).

### Ultimate Testing Machine (UTM)

The ultimate tensile strength of the designed nanohydrogel film series (CSG) was measured by a universal testing machine (AG-20KNXD Plus, Shimadzu). The hydrogel slices had a 2.5-inch length and breadth of 0.5 inches. The testing method was in accord with ASTM D412-98A. The gage length (1.60 inches) as well as the speed of the crosshead 5.0mm/min was set. Ultimate tensile strength was calculated in MPa simply by dividing the force (F) to split the film over the film sample's area (A). It also measured the percentage elongation at break (in % E) and estimated the average of at least three UTS determinations and percentage E.

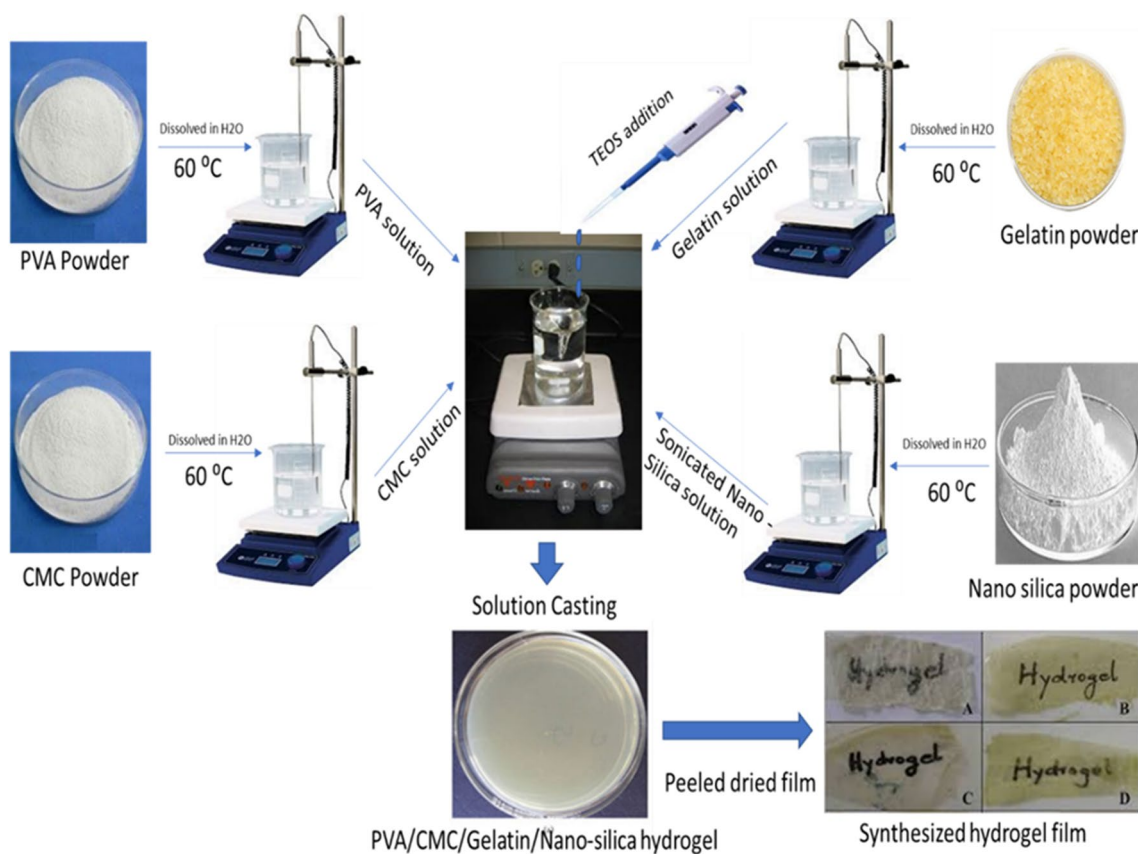


Fig. 1 Schematic representation of CSG hydrogel film preparation

### Swelling Test (ST)

In distilled water, the biodegradable hydrogel base film sample's swelling testing was examined. Cut the dried film sample (0.025g pre-weighted) into small pieces from a plastic petri dish and then load that dish with 80mL distilled water. The abundance of water weight of the film was measured after each 10min. The swollen sample was then placed in the water again till the establishment of equilibrium occurred. All experiments were repeated into triplets and the average results have been considered. By assigned relation, the swelling ratio for samples was calculated by Eq. (1).

$$\text{Degree of Swelling} = \frac{W_s - W_d}{W_d} \quad (1)$$

Where,  $W_s$  = Swollen weight of the film and  $W_d$  = Dry weight of the film

The swelling mechanism of the CSG series for water diffusion was evaluated by Eq. (2).

$$F = kt^n \quad (2)$$

Where F represents the fractional swelling at time t (min) that is calculated by the swelling ratio of  $W_t$  and  $W_{eq}$ .  $W_{eq}$

and  $W_t$  are equilibrium swelling ratios at time t and k is the swelling rate constant, while n is the diffusion exponent that helps to find the release mechanism. The degree of swelling of the CSG series was used to analyze the values of n and k.

### Applications of the Hydrogel Film

#### Antioxidant Activity

The standard solution of DCPIP was prepared by taking 0.024g of salt in a piece of aluminium foil in the dark and dissolved in 50mL  $C_2H_5OH$ . The prepared solution is then transferred to a 100mL volumetric flask and up to the mark the volume with absolute ethanol, this solution will be the standard solution of 1000 $\mu$ g/mL. The absorbance of the control was analyzed at 517nm. The standard antioxidant (Vitamin C) with different concentrations: i.e. 50,100,150,200,250,300 and 350 $\mu$ g/mL. The solutions were incubated for 30min at 25 $^{\circ}$ C in the dark. The inhibition rate was measured at 517nm. All experiments were repeated into triplets and the average results have been considered. The antioxidant rate was determined by Eq. (3).



$$\% \text{ Inhibition} = \left( \frac{\text{Abs of control} - \text{Abs of sample}}{\text{Abs of control}} \right) \times 100 \quad (3)$$

The sample solutions of the hydrogels were prepared by considering a circular diameter of 3cm in 10mL of methanol (0.1mM in methanol) and shaking them in a water bath for 1h. 1mL of prepared hydrogel sample was mixed with 3mL of DCPIP. After 30min of keeping in the dark, the absorbance of all the standard (vitamin C) and hydrogel samples was measured at 517nm. The scavenging % was determined by Eq. (4) [17].

$$\% \text{ Scavenging Activity} = \left( \frac{\text{Abs of blank} - \text{Abs of sample}}{\text{Abs of blank}} \right) \times 100 \quad (4)$$

### Antimicrobial Activity

The antibacterial activity was analyzed by the agar disc diffusion method. A nutritional medium for the development of bacterial strains was prepared to test the antibacterial properties of hydrogels. The agar solution was prepared following the standard method while agar was dissolved in distilled water was shaken thoroughly for proper mixing. The agar solution-containing bottle was covered with aluminium foil and autoclaved to sterilize the agar, ensuring that no other microorganisms except the selected one could thrive. The autoclave was performed at 120°C for 20min. After 20min of autoclave, once the temperature was down to 60°C, the agar solution bottle was placed under laminar flow. Following that, agar was placed into the plates, letting them cool down to set on the plates. Sanitized cotton swabs were used to spread a little bacterial culture across the plates. On the plates, two different bacterial strains, gram-positive *B. cereus* and gram-negative *E. coli* were grown in separate petri dishes with the use of a sterile cotton swab. Using sterile tweezers, five disc-shaped hydrogels were placed on the agar plates. The discs' diameter was maintained at 6mm. Plates were kept upside down at 37°C for around 24h while being maintained culture growth. The limiting area of the culture plates was determined by measuring them [18]. All experiments were repeated into triplets and the average results have been considered.

### Soil Burial Test

The biodegradability of the designed nanohydrogel film series (CSG) was measured by a soil burial test [19]. The film samples were cut into 20x40mm size, weighed and then buried in soil which is in a container with a depth of 10cm. Well sprinkling water on the soil to maintain enough humidity and check with regular time intervals. The effect of soil

and its' humidity was observed after a one-week interval of time and the CSG film was washed gently with distilled water to remove any soil from them. The CSG hydrogels were then dried and weighed. The samples were then buried again and the same procedure was repeated for 5 weeks and mass was taken after every week. All experiments were repeated into triplets and the average results have been considered. The biodegradation of the CSG nano hydrogel film samples was then calculated using Eq. (5).

$$\text{Mass Loss (\%)} = \frac{m_i - m_f}{m_i} \times 100 \quad (5)$$

Where  $m_d$  is the dried weight of the polymer blend film and  $m_i$  is the initial weight of CSG hydrogel polymer blend film.

## Results and Discussion

### Spectral Studies of CSG Hydrogel

The presence of the carboxyl group (-COOH) in carboxymethyl cellulose presented in Fig. 2 showed a prominent absorption band at 1593cm<sup>-1</sup>. The stretching frequency of the -OH group is visible in the broad absorption band at 3284cm<sup>-1</sup>. At 2913cm<sup>-1</sup>, the C-H group's stretching vibration is visible. The vibration of -CH<sub>2</sub> scissoring at 1486cm<sup>-1</sup> and -OH bending at 1348.34cm<sup>-1</sup>, respectively, are ascribed to these bands. The CH-O-CH<sub>2</sub> band at 1046cm<sup>-1</sup> exhibits its stretching [20]. The O-H stretching vibration of the polymer and water involved in hydrogen bonding is represented by the absorption peak of cellulose in the region of

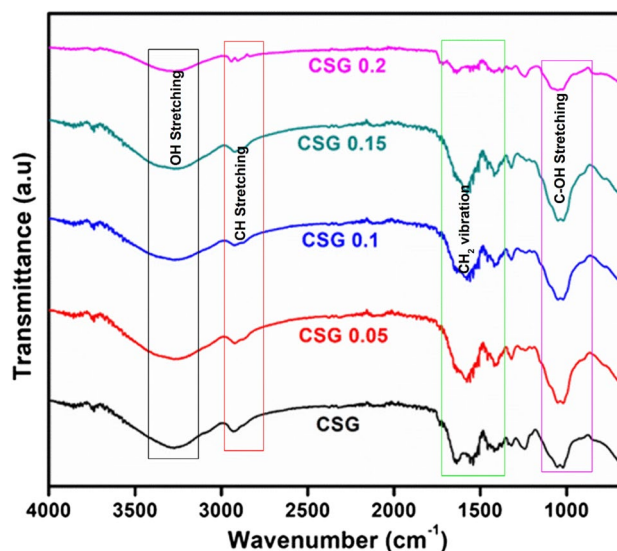


Fig. 2 FTIR spectra of CSG hydrogel films

3114–3661 $\text{cm}^{-1}$ . Stretching modes for C-H can be seen in the area of FTIR spectra between 2831 $\text{cm}^{-1}$  and 2989 $\text{cm}^{-1}$ . It was also noted that the region of about 1473 $\text{cm}^{-1}$  was deformed by  $-\text{CH}_2$ . 1015 $\text{cm}^{-1}$  has a range of pyranose rings. Because of their monosaccharide molecules containing pyranose rings, the range of 1015 $\text{cm}^{-1}$  can be explained. Cellulose's C-H, C-O, and C-OH stretching infrared absorption spectroscopy in the 817–1166 $\text{cm}^{-1}$  band [21].

PVA is associated with the stretching O-H from the intramolecular and intermolecular hydrogen bonds because of the broad bands between 3600–3000 $\text{cm}^{-1}$ . The vibrational band seen between 2857 $\text{cm}^{-1}$  is due to the stretching of C-H from alkyl groups, and the peaks between 1750–1720 $\text{cm}^{-1}$  are caused by the stretching of C=O from the acetate group still present in PVA [20]. Since its monosaccharide contains pyranose rings, the range of 1015  $\text{cm}^{-1}$  can be explained. The existence of both Si-O-Si and Si-O-C was revealed by the asymmetric stretching bands in the 1105–1015 $\text{cm}^{-1}$  range, which supported the crosslinking via silanol (Si-OH) groups. In the produced hydrogels, OH stretching of intra- and intermolecular hydrogen bonds was visible in a wide region between 3550–3150 $\text{cm}^{-1}$ . At 2921 $\text{cm}^{-1}$ , an alkyl group vibrational band ( $-\text{CH}$  stretching) was noticed. At 3710 $\text{cm}^{-1}$ , the Si-OH stretching vibration was observed [20].

### Structural Studies of CSG Hydrogels

The X-ray diffraction (XRD) technique is important for analyzing the structural characteristics of the sample under examination. The technique of X-ray diffraction is also used to evaluate the dispersion of incorporated particles in film samples. Plotting an X-ray diffraction chart between two theta values and intensity in counts, where two thetas are taken across the x-axis and intensity along the y-axis. The X-ray wavelength is between 0.1–100 angstrom and the X-ray is considered to be electromagnetic radiation. Dispersion of  $\text{SiO}_2\text{NPs}$  was investigated by X-ray diffraction patterns in polymer structure. Results revealed in Fig. 3 that the CSG sample prepared with natural polymers, due to its amorphous behaviour indicated no peak in the pattern [22, 23]. The reinforcement of different amounts of  $\text{SiO}_2\text{NPs}$  (filler) in hydrogel film samples showed their crystalline behaviour because particles of  $\text{SiO}_2\text{NPs}$  tangled between the chains of the polymers and increasing the concentration of  $\text{SiO}_2\text{NPs}$  in samples increased their crystallinity. It was also observed that when the concentration of  $\text{SiO}_2\text{NPs}$  increased in film samples this increased the intensity at a fixed angle. Results showed samples CSG 0.15 and CSG 0.2 revealed high crystalline behaviour with maximum intensity and could not handle and carry the food item. Thus, sample CSG 0.1 with appropriate crystallinity and flexibility is preferred for food packaging film.

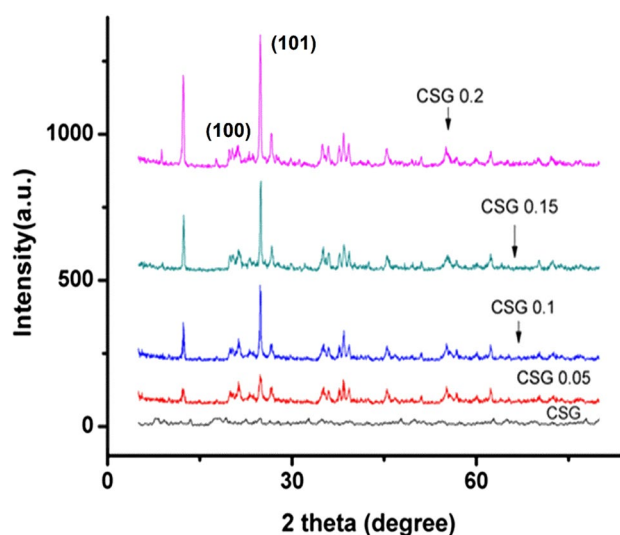


Fig. 3 Diffractogram results of CSG hydrogel films

### Surface Morphology of CSG Hydrogel Films

Scanning electron microscopy (SEM) is important for studying the surface morphology of the CSG hydrogel films. SEM micrographs give information about pore size, polymeric structure as well and entanglement of particles ( $\text{SiO}_2\text{NPs}$ ) with pores of hydrogel films. All the film samples consisted of the same polymeric concentration (PVA/CMC/gelatin) but different concentrations of  $\text{SiO}_2\text{NPs}$ . SEM micrographs showed that film sample CSG (without  $\text{SiO}_2\text{NPs}$ ) exhibited prominent pores surface presented in Fig. 4(a, b). The surface of the film sample CSG 0.05 (with 0.05g  $\text{SiO}_2\text{NPs}$ ) becomes a uniform reduction in pore size due to the presence of  $\text{SiO}_2\text{NPs}$  with nanoscale interaction with chains of polymers as in Fig. 4(c, d). As the concentration of  $\text{SiO}_2\text{NPs}$  (0.1g) was increased in film sample of CSG 0.1, then micrographs were observed along with evenly distributed  $\text{SiO}_2\text{NPs}$  with lessening the average pore size as shown in Fig. 4(e, f). Also, the further addition of  $\text{SiO}_2\text{NPs}$  0.15g and 0.2g in hydrogel film samples, CSG 0.15 and CSG 0.2, respectively, showed the large, deformed patches which presented the fractured surface a coarse appearance Fig. 4(g, h & i, j). SEM micrographs also revealed that increasing the concentration of  $\text{SiO}_2\text{NPs}$  in hydrogel films decreases the pore size of hydrogel films. It was clearly observed that the film sample, CSG 0.1 with favourable surface morphology, appropriate pore size and appropriate crystallinity can be preferred as a supportive format for food packages.

### Thermal Analysis of CSG Hydrogel Films

TG thermograms in Fig. 5 revealed that the film samples with  $\text{SiO}_2\text{NPs}$  required more temperature for thermal

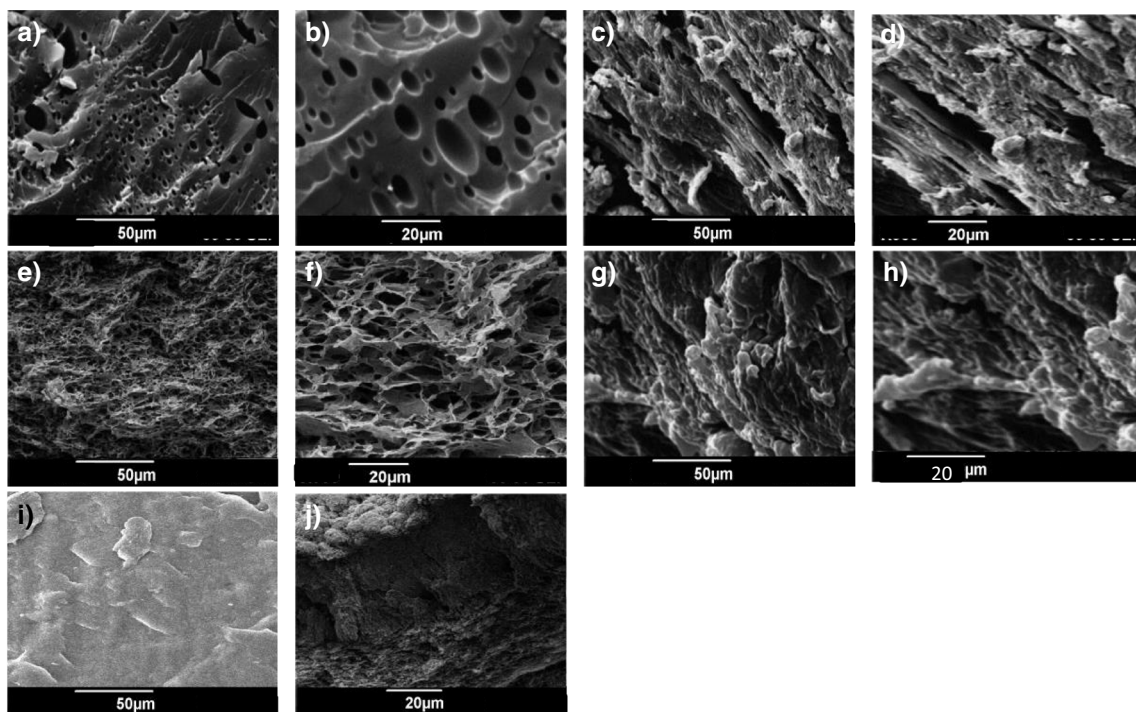


Fig. 4 Micrographs of CSG hydrogel films

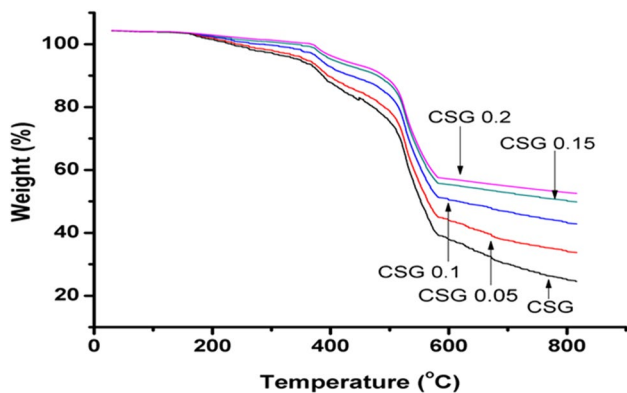


Fig. 5 TGA results of CSG hydrogel films

degradation, so the incorporation of SiO<sub>2</sub>NPs provided thermally stable films. The differential thermal analysis provides information about endothermic or exothermic changes that take place in the material under examination. In the present case, endothermic changes are revealed by prepared film samples with the addition of SiO<sub>2</sub>NPs. The results of differential thermal analysis of prepared hydrogel film samples presented in Fig. 6 showed that each pattern revealed three endothermic peaks at approximately 345°C, 534°C and 615°C. All thermograms revealed that physical changes occurred in prepared film samples with the incorporation of SiO<sub>2</sub>NPs.

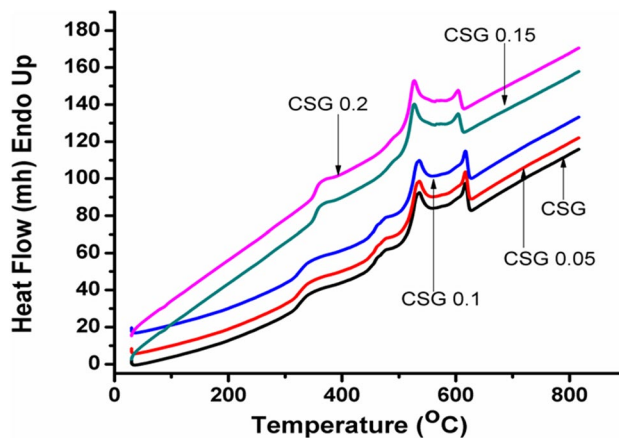


Fig. 6 DTA results for prepared blended CSG hydrogel films

### Mechanical Strength Analysis of CSG Hydrogel Films

Food packaging films demand durability to withstand stress during the packing and handling of food products. The concentration of SiO<sub>2</sub>NPs in the prepared film samples affects the tensile strength significantly; it supports the polymer network in Fig. 7 and Table 2. It was observed that increasing the concentration of SiO<sub>2</sub>NP exhibited improvement in the ultimate tensile strength of prepared film samples. This revealed that with the

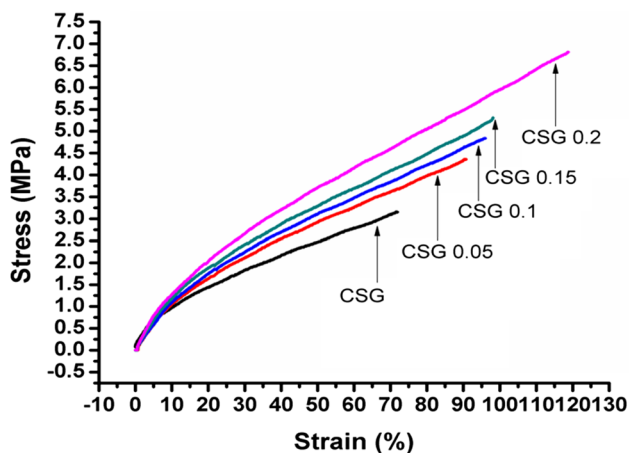


Fig. 7 UTS results for prepared blended CSG hydrogel films

Table 2 Ultimate tensile strength and percentage elongation at break of CSG hydrogel films

Sample codes	Ultimate tensile strength (MPa)	Elongation at break (%)
CSG	3.15	72
CSG 0.05	4.35	90
CSG 0.1	4.83	96
CSG 0.15	5.31	98
CSG 0.2	6.81	118

inclusion of the filler, a greater force was needed to break the film sample. Especially for the film sample with higher SiO<sub>2</sub>NPs (filler) concentration showed the highest ultimate tensile strength.

### Swelling and Diffusion Test of CSG Hydrogel Films

The distilled water was used for the measurement of the swelling activity of the prepared film samples. The swelling behaviour of film samples was estimated in the water until the equilibrium was reached. The film samples exhibited continuous increasing swelling activity with time Fig. 8. Results represented those increasing concentrations of SiO<sub>2</sub>NPs in film samples CSG 0.05, CSG 0.1, CSG 0.15 and CSG 0.2 increased their swelling behavior. The equilibrium time of CSG, CSG 0.05, CSG 0.1, CSG 0.15 and CSG 0.2 was 70, 70, 100,70 and 80min, respectively. Results revealed hydrogel film CSG 0.1 is more stable than other samples, so hydrogel film CSG 0.1 is good for food packages.

The plot between ln F versus ln t is represented in Fig. 9 and the parameters of diffusion are elaborated in Table 3. CSG, CSG 0.05, CSG 0.15 and CSG 0.2 followed the Fickian

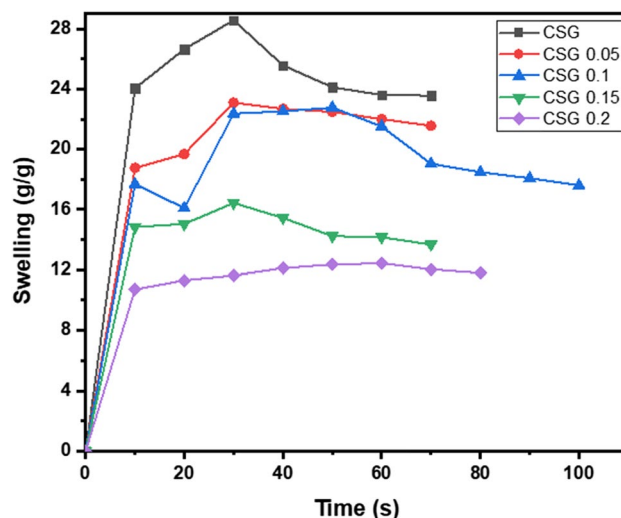


Fig. 8 Swelling test results for prepared blended CSG hydrogel films

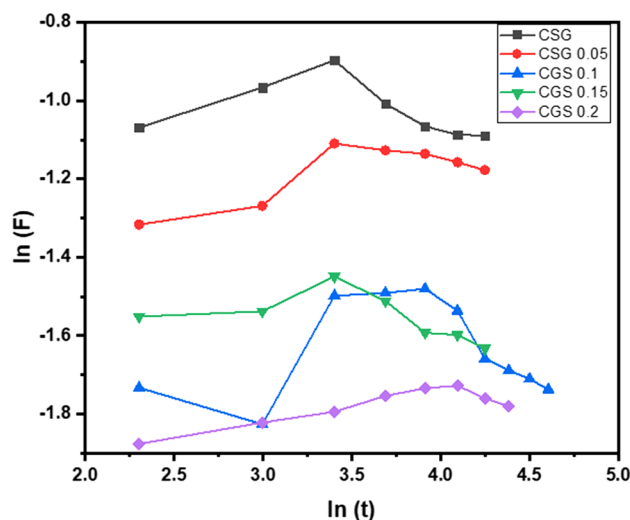


Fig. 9 Diffusion responses for CSG hydrogels films

Table 3 Diffusion parameters of CSG hydrogel films

Parameters	CSG	CSG 0.05	CSG 0.1	CSG 0.15	CSG 0.2
n	0.23	1.30	0.80	0.31	0.104
Intercept	-1.40	-3.82	-2.54	-1.17	-0.24
K	0.24	0.021	0.07	0.31	0.78
Regression (R %)	92	85	83	99	96

diffusion phenomenon because the value of n < 0.5 meant there was an active water penetration due to a higher rate of relaxation than the rate of diffusion. CSG 0.1 showed non-Fickian diffusion behaviour as the value of n > 0.5 (0.80) which means, the water penetration rate was higher than



the rate of polymeric chains relaxation, whereas CSG 0.05 showed a super case II diffusion mechanism as the value of  $n$  was greater than 1 (1.30).

### Antioxidant Activity

Antioxidant activity of the CSG series was performed by simple method by using free radical of DCPIP. This antioxidant test is the most acknowledged method for assessing the free radical scavenging activity of hydrogel [24]. This method is extensively used to investigate the ability of hydrogels to behave as free radical scavengers/hydrogen donors and to assess antioxidant activity [25]. Antioxidant behavior is mainly based on the reduction behavior of DCPIP which gives maximum absorption at 517nm due to the odd number of electrons [26]. When the solution sample hydrogels react with DCPIP solution, the hydrogel sample turns paired in the presence of H-donor (which is the free radical scavenging activity of hydrogels) and it is reduced in the form of DCPIP-H. Due to reduction, the absorbance of hydrogels decreased as compared to the pure DCPIP [27]. The sample hydrogels of the CSG series displayed the increasing order of their antioxidant action [28]. The radicals that form DCPIP-H, mainly depend on the number of the electrons captured by the hydrogel H-donor [25, 29]. The intermolecular H-bonds also are formed among SiO<sub>2</sub>NPs and other film production compounds which accelerate the anti-oxidant properties into the film [30]. CSG has lower antioxidant activity as compared to others, the addition of a strong antioxidant such as promises to demonstrate much greater improvement with the addition of SiO<sub>2</sub>NPs [31, 32]. By increasing the amount of SiO<sub>2</sub>NPs the hydrogels represented the increase in antioxidant activity as depicted in Fig. 10 and the absorbance measure is tabulated in Table 4 [33, 34].

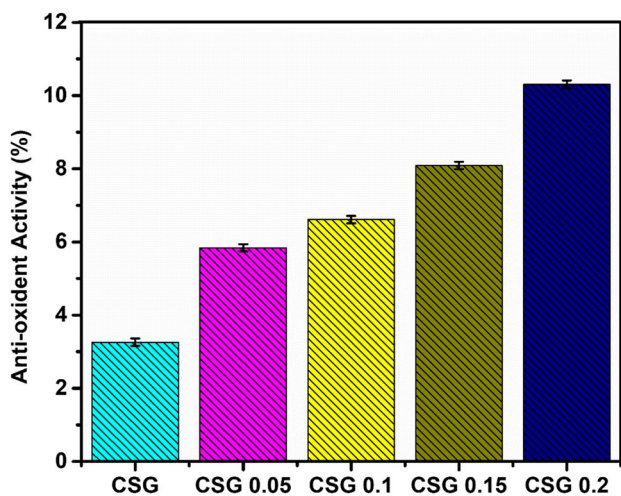


Fig. 10 Antioxidant activity of blended CSG hydrogel films

Table 4 Absorbance measurements of CSG hydrogel films

Sample code	Absorbance (nm)
CSG	2.537
CSG 0.05	2.691
CSG 0.1	2.756
CSG 0.15	2.742
CSG 0.2	2.736

### Antimicrobial Activity

To corroborate the drug release studies, antimicrobial activity was carried out to inter-relate the zone of inhibition of microbial growth with hydrogels. The study was performed by disc diffusion method by using the hydrogel sample of 6mm diameter against *B. cereus* and *E. coli* that was used as a bacterial model [35]. All the hydrogels exhibited the zone of inhibition of different centimetres. According to Table 5, every CSG hydrogel film inhibited its growth against *E. coli* and *B. cereus*. The empty areas on the agar plates with varying sizes demonstrated the effectiveness of the hydrogels for microbial resistance. The CSG hydrogel's inhibitory zone was minimal, but as the crosslinker concentration was increased, the CSG series displayed a reasonable amount of antimicrobial action. CSG 0.1 and CSG 1.5 both exhibited antimicrobial activity up to 0.5cm and 0.4cm in diameter respectively, but CSG and CSG 0.05 had inhibition zones of 0.2cm and 0.4cm, respectively presented in Fig. 11(a). On the other hand, CSG 0.1 and CSG 1.5 both exhibited antimicrobial activity up to 1.2-1.5cm in diameter, respectively, but CSG and CSG 0.05 had inhibition zones of 0.4cm and 1.1cm, respectively presented in Fig. 11(b). SiO<sub>2</sub>NPs-modified CSG films have significant influence on antibacterial activity due to its' characteristics such as hydrophobia, oleophobia, a cationic nature, resistance to acids, excellent flexibility, and resistance to abrasion and corrosion which inhibits adhesion and proliferation of microorganisms [36–39].

### Soil Burial Response

Biodegradability of the designed CSG hydrogel films was observed using a soil burial environment having moisturized and nourished conditions. The 25°C temperature of the moisturized environment was observed which was

Table 5 Antibacterial activity (diameter of inhibition zone) of CSG hydrogel films

Bacteria type	CSG (cm)	CSG 0.05 (cm)	CSG 0.1 (cm)	CSG 0.15 (cm)
<i>B. cereus</i>	0.4	0.9	1.2	1.5
<i>E. coli</i>	0.2	0.4	0.5	0.4

**Fig. 11** Antibacterial activity of blended CSG hydrogel films towards

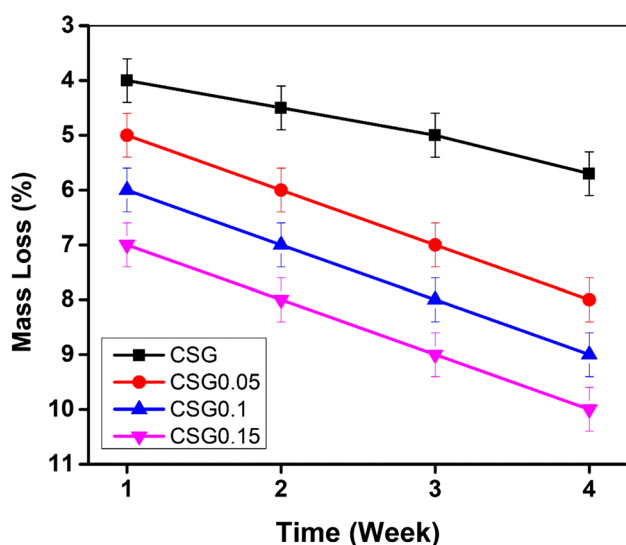
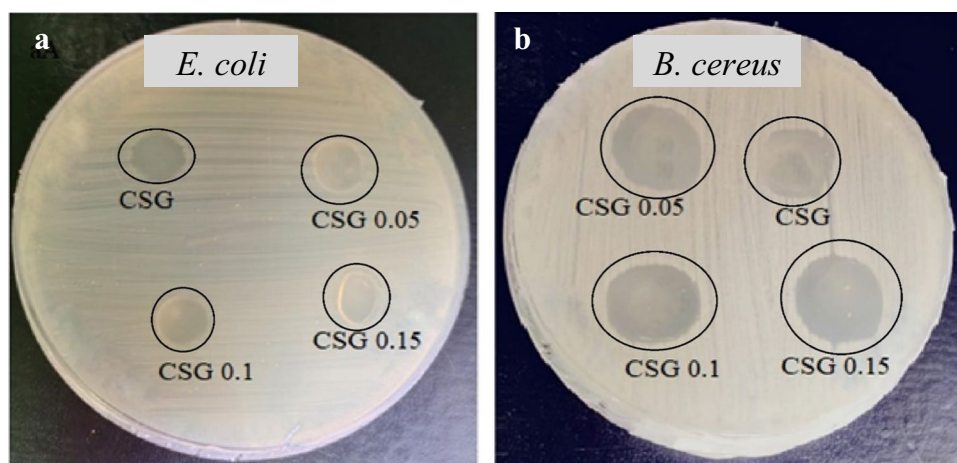


**Fig. 12** Effect of time on biodegradability of PVA/gelatin hydrogel films

satisfactory for the development of microorganisms' habitat that may play a dynamic part in the biodegradation of CSG hydrogel films. The CSG film samples were placed in the soil for 5 weeks and examined after each week. Figure 12 depicts the behaviour of different CSG films under the soil with a one-week time interval.

The neat CSG hydrogel films without reinforcement of  $\text{SiO}_2\text{NPs}$  exhibited more mass loss than any other CSG-reinforced hydrogel films. Hence, it is apparent that mass loss declined as the amount of nano reinforcement was enhanced. Therefore, increasing the amount of nanofiller, the mass loss was rapid. Initially, the mass loss rate was lessened in the first one-week period and the trend is the same for all hydrogel films; but after that, the rate of biodegradation increased sharply. This phenomenon occurred because of the polymeric nature of hydrogel film as the polymeric chain

breakage started, the role of reinforced nano-reinforcements initiated acting and that provided the space and favourable environment for microorganisms to proliferate and initiate degradation of CSG hydrogel films which presented its' high potential to be used as a substitute packaging material.

## Conclusions

The present study involved the preparation of novel food packaging films using gelatine, CMC, PVA, and  $\text{SiO}_2\text{NPs}$  crosslinked with TEOS. The addition of  $\text{SiO}_2\text{NPs}$  resulted in enhanced thermal and mechanical strength of the film samples. XRD analysis revealed distinct peaks corresponding to the presence of  $\text{SiO}_2\text{NPs}$  in the prepared films, with an increase in crystallinity observed with higher concentrations of  $\text{SiO}_2\text{NPs}$  at a fixed angle. SEM analysis indicated that the pore size of the hydrogel films decreased with increasing  $\text{SiO}_2\text{NPs}$  concentration. Among the film samples, CSG 0.1 exhibited favourable surface morphology and an appropriate pore size, leading to low weight and high specific surface area. This characteristic provides interesting opportunities for mechanical protection, thermal insulation, and adsorbing or releasing specific compounds that make it suitable for food packaging applications. TGA/DTA results demonstrated that the thermal stability of the prepared film samples improved with increasing  $\text{SiO}_2\text{NPs}$  concentration. UTS analysis revealed that the mechanical strength of the film samples was enhanced by higher concentrations of  $\text{SiO}_2\text{NPs}$ , but it displayed high crystallinity which is unfavourable for swelling characteristics of biodegradable hydrogels. Therefore, the film sample CSG 0.1, with an appropriate  $\text{SiO}_2\text{NPs}$  concentration of 0.1g, displayed 96% elongation at break and 4.8MPa ultimate tensile strength, offering flexibility with moderate crystallinity, making it a suitable supportive format for food packaging purposes. Furthermore, the swelling activity of the hydrogel films in water was highest

for the CSG 0.1 film sample, attributed to the appropriate concentration of 0.1g of SiO<sub>2</sub>NPs, which increased the film's swelling capacity. These findings highlight the suitability of CSG 0.1 for food packaging applications, considering its favourable thermo-mechanical properties. Strong nature of biodegradability was observed with the utmost loading of nano reinforcement. To conclude, the film sample CSG 0.1 can be recommended for food packaging purposes due to its desirable characteristics. The overall cost-effectiveness of this biofilm, market feasibility, environmental impacts, and comparative study with commercial synthetic plastic are highly recommended to be assessed in further studies.

**Author Contribution** SS- Conceptualization, Writing (Original Draft), UK, WA, MK-Methodology and Formal Analysis, NH- Writing (Original Draft).

**Funding** Open Access funding enabled and organized by CAUL and its Member Institutions This research work was funded by Institutional Fund Projects under grant no. (IFPIP: 687-829-1443).

**Data availability** The data that support the findings of this study are available from the corresponding author, Nazia Hossain, upon reasonable request.

## Declarations

**Ethics approval and consent to participate** The facts and views in the manuscript are solely ours, and we are totally responsible for authenticity, validity, and originality. We also declare that this manuscript is our original work, and we have not copied from anywhere else. There is no plagiarism in my manuscript.

**Consent for publication** We undertake and agree that the manuscript submitted to your journal has not been published elsewhere and has not been simultaneously submitted to other journals.

**Competing interests** The authors declare no conflict of interest.

**Open Access** This article is licensed under a Creative Commons Attribution 4.0 International License, which permits use, sharing, adaptation, distribution and reproduction in any medium or format, as long as you give appropriate credit to the original author(s) and the source, provide a link to the Creative Commons licence, and indicate if changes were made. The images or other third party material in this article are included in the article's Creative Commons licence, unless indicated otherwise in a credit line to the material. If material is not included in the article's Creative Commons licence and your intended use is not permitted by statutory regulation or exceeds the permitted use, you will need to obtain permission directly from the copyright holder. To view a copy of this licence, visit <http://creativecommons.org/licenses/by/4.0/>.

## References

1. N. P. Mahalik and A. N. Nambiar (2010). Trends in food packaging and manufacturing systems and technology. *Trends in food science & technology* **21** (3), 117–128.
2. K. Li, et al. (2019). Bioinspired interface engineering of gelatin/cellulose nanofibrils nanocomposites with high mechanical performance and antibacterial properties for active packaging. *Composites Part B: Engineering* **171**, 222–234.
3. S. Farris, et al. (2009). Development of polyion-complex hydrogels as an alternative approach for the production of bio-based polymers for food packaging applications: a review. *Trends in food science & technology* **20** (8), 316–332.
4. A. K. Singh, P. Itkor, and Y. S. Lee (2023). State-of-the-Art Insights and Potential Applications of Cellulose-Based Hydrogels in Food Packaging: Advances towards Sustainable Trends. *Gels* **9** (6), 433.
5. L.-L. Liu, et al. (2015). Structural diversity and photocatalytic properties of Cd (II) coordination polymers constructed by a flexible V-shaped bipyridyl benzene ligand and dicarboxylate derivatives. *Dalton Transactions* **44** (4), 1636–1645.
6. Y. Bao, et al. (2022). Functionalization and antibacterial applications of cellulose-based composite hydrogels. *Polymers* **14** (4), 769.
7. P. Dutta, et al. (2009). Perspectives for chitosan based antimicrobial films in food applications. *Food chemistry* **114** (4), 1173–1182.
8. Y. Ahmadian, et al. (2019). Synthesis of polyvinyl alcohol/CuO nanocomposite hydrogel and its application as drug delivery agent. *Polymer Bulletin* **76** (4), 1967–1983.
9. P. N. Charron, T. A. Braddish, and R. A. Oldinski (2019). PVA-gelatin hydrogels formed using combined theta-gel and cryo-gel fabrication techniques. *Journal of the mechanical behavior of biomedical materials* **92**, 90–96.
10. B. Krishnakumar, et al. (2018). Highly active P25@ Pd/C nanocomposite for the degradation of Naphthol Blue Black with visible light. *Journal of Molecular Structure* **1153**, 346–352.
11. Zhang, W., et al., *Role of silica (SiO<sub>2</sub>) nano/micro-particles in the functionality of degradable packaging films/coatings and their application in food preservation*. Trends in Food Science & Technology, 2023.
12. S. Murali, et al. (2019). Bio-based chitosan/gelatin/Ag@ ZnO bionanocomposites: synthesis and mechanical and antibacterial properties. *Cellulose* **26**, 5347–5361.
13. A. C. Batista, et al. (2010). Distinctive clinical and microscopic features of squamous cell carcinoma of oral cavity and lip. *Oral Surgery, Oral Medicine, Oral Pathology, Oral Radiology, and Endodontology* **109** (3), e74–e79.
14. S. Sagar, et al. (2022). Synergistic influence of tetraethyl orthosilicate crosslinker on mixed matrix hydrogels. *Applied Nanoscience* **12** (10), 2923–2932.
15. S. Kumar, et al. (2019). Bio-based (chitosan/PVA/ZnO) nanocomposites film: Thermally stable and photoluminescence material for removal of organic dye. *Carbohydrate Polymers* **205**, 559–564.
16. C. Zhang, et al. (2020). Eco-friendly bioinspired interface design for high-performance cellulose nanofibril/carbon nanotube nanocomposites. *ACS Applied Materials & Interfaces* **12** (49), 55527–55535.
17. S.-B. Park, et al. (2017). Biopolymer-based functional composites for medical applications. *Progress in Polymer Science* **68**, 77–105.
18. Hudzicki, J., *Kirby-Bauer disk diffusion susceptibility test protocol*. 2009.
19. M. Zeeshan, et al. (2021). Synergistic effect of silane cross-linker (APTEOS) on PVA/gelatin blend films for packaging applications. *High Performance Polymers* **33** (7), 815–824.
20. S. Jabeen, et al. (2017). Development of a novel pH sensitive silane crosslinked injectable hydrogel for controlled release of neomycin sulfate. *International journal of biological macromolecules* **97**, 218–227.
21. Cao, Y., et al. *Effect of micronization on the structure and particle size of guar gum*. in *IOP Conference Series: Earth and Environmental Science*. 2018. IOP Publishing.

22. Maiti, B., et al., *Thermoresponsive Shape-Memory Hydrogel Actuators Made by Phototriggered Click Chemistry*. Advanced Functional Materials, 2020: p. 2001683.
23. S. Sagar, et al. (2015). Fabrication and thermal characteristics of functionalized carbon nanotubes impregnated polydimethylsiloxane nanocomposites. *Journal of Composite Materials* **49** (8), 995–1006.
24. S. Pulipati, et al. (2017). Determination of total phenolic, tannin, flavonoid contents and evaluation of antioxidant property of *Amaranthus tricolor* (L). *International Journal of Pharmacognosy and Phytochemical Research* **9** (6), 814–819.
25. L. Leaves and L. Leaves (2014). Antioxidant activity by DPPH radical scavenging method of *ageratum conyzoides*. *American Journal of Ethnomedicine* **1** (4), 244–249.
26. P. Warriar, V. Nambiar, and C. Ramankutty, *Indian Medicinal Plants: A Compendium of 500 species Orient Longman Publishers*. (Kottakkal, India, 1994), p. 2.
27. S. Handa, D. Rakesh, and K. Vasisht (2006). Compendium of medicinal and aromatic plants ASIA. *ICS UNIDO Asia* **2**, 305.
28. Harborne, A., *Phytochemical methods a guide to modern techniques of plant analysis*. 1998: springer science & business media.
29. D. S. Priya, et al. (2015). Antioxidant activity of the simple ascidian *Phallusia nigra* of Thoothukudi Coast. *International Journal of Pharmaceutical Chemistry* **12**, 410–412.
30. W. Dong, et al. (2022). Characterization and antioxidant properties of chitosan film incorporated with modified silica nanoparticles as an active food packaging. *Food Chemistry* **373**, 131414.
31. S. Farhangi-Abriz and S. Torabian (2018). Nano-silicon alters antioxidant activities of soybean seedlings under salt toxicity. *Protoplasma* **255** (3), 953–962.
32. X. Gao, et al. (2008). Antioxidant behaviour of a nanosilica-immobilized antioxidant in polypropylene. *Polymer degradation and stability* **93** (8), 1467–1471.
33. M. E. Abdel-Haliem, et al. (2017). Effect of silica ions and nano silica on rice plants under salinity stress. *Ecological Engineering* **99**, 282–289.
34. L. Valgimigli, A. Baschieri, and R. Amorati (2018). Antioxidant activity of nanomaterials. *Journal of Materials Chemistry B* **6** (14), 2036–2051.
35. S. Khade, et al. (2014). Gelatin-PEG based metronidazole-loaded vaginal delivery systems: preparation, characterization and in vitro antimicrobial efficiency. *Iranian Polymer Journal* **23** (3), 171–184.
36. R. Lacerda-Santos, et al. (2020). In vivo biocompatibility of silicon dioxide nanofilm used as antimicrobial agent on acrylic surface. *Anais da Academia Brasileira de Ciências* **92**, e20181120.
37. D. Camporotondi, et al. (2013). Antimicrobial properties of silica modified nanoparticles. *Microbial pathogens and strategies for combating them: science, technology and education* **2**, 283–290.
38. N. Hossain, et al. (2024). Synthesis, performance and reaction mechanisms of Ag-modified multi-functional rice husk solvochar for removal of multi-heavy metals and water-borne bacteria from wastewater. *Process Safety and Environmental Protection* **182**, 56–70.
39. A. Ahmad, et al. (2022). Novel antibacterial polyurethane and cellulose acetate mixed matrix membrane modified with functionalized TiO<sub>2</sub> nanoparticles for water treatment applications. *Chemosphere* **301**, 134711.

**Publisher's Note** Springer Nature remains neutral with regard to jurisdictional claims in published maps and institutional affiliations.